An HTS X-Band DC SQUID Based Amplifier: Modeling and Development Concepts

Georgy V. Prokopenko, Sergey V. Shitov, Igor V. Borisenko, and Jesper Mygind

***Abstract*—We present an X-band amplifier concept based on a HTS grain boundary dc SQUID, which allow for extended dynamic range for use with SIS mixers, e.g., as a buffer amplifier in front of an RSFQ ADC, or possibly for satellite and cellular phone communications. The proposed rf design is based on a combination of single-layer slot and coplanar lines forming novel input and output circuits. The following parameters (per stage) are obtained via simulation for central frequency 11 GHz: bandwidth 0.5–1 GHz, power gain 11–12 dB, noise temperature 5–10 K. A saturation product as high as 500–1000 K·GHz is estimated for a characteristic voltage of 1–2 mV. The realization of these parameters makes HTS SQA competitive with existing coolable HEMT-amplifiers for radio astronomy and satellite communication.**

***Index Terms*—Josephson devices, RF amplifiers, superconducting devices, superconducting quantum interference devices.**

I. Introduction

THE dc SQUID based rf amplifier (SQA) with HTS bicrystal junctions is a promising device due to its high characteristic voltage, V_C, which may enhance the dynamic range of the SQA [1]. According to recent tests [2], [3] a low-noise dc SQUID based rf amplifier made from low-T_C materials has a fairly low saturation power, and can be saturated with a wide-band noise signal of equivalent temperature of 150 K or even lower. This can be associated with low characteristic voltage $V_C = I_C R_N$, where I_C is the critical current and R_N is the normal state resistance of the SQUID. It is found convenient to present the saturation power as the temperature of the white noise, $T_{\rm SAT}$, occupying the band of 1 GHz: $T_{\rm SAT}^{1\ \rm GHz} \approx V_B^2/(8R_D \cdot k_B \cdot \Delta f \cdot G_{\rm SQA})$. Here V_B is the bias voltage of SQA, R_D is the dynamic resistance, k_B is Boltsman's constant, Δf is the bandwidth equal to 1 GHz, $G_{\rm SQA}$ is the power gain. This formula assumes that the bias point V_B defines the maximum voltage amplitude along the 'linear' branch of the I-V curve. The maximum span of this 'linear' branch may be characterized by V_C, which usually does not exceed 300 μV for 1 μm^2 area low-T_C junctions. To increase the saturation power one needs junctions with higher V_C assuming that optimum bias point can be set at $V_B = V_C/2$. The characteristic voltage of HTS junctions can be as high as 10 mV at 4.2 K [5], [6]. This is why the dc SQUID rf amplifiers made from high-T_C materials can be very promising devices for a number of practical low-noise applications where small size and extremely low power dissipation are important along with necessity of a high dynamic range.

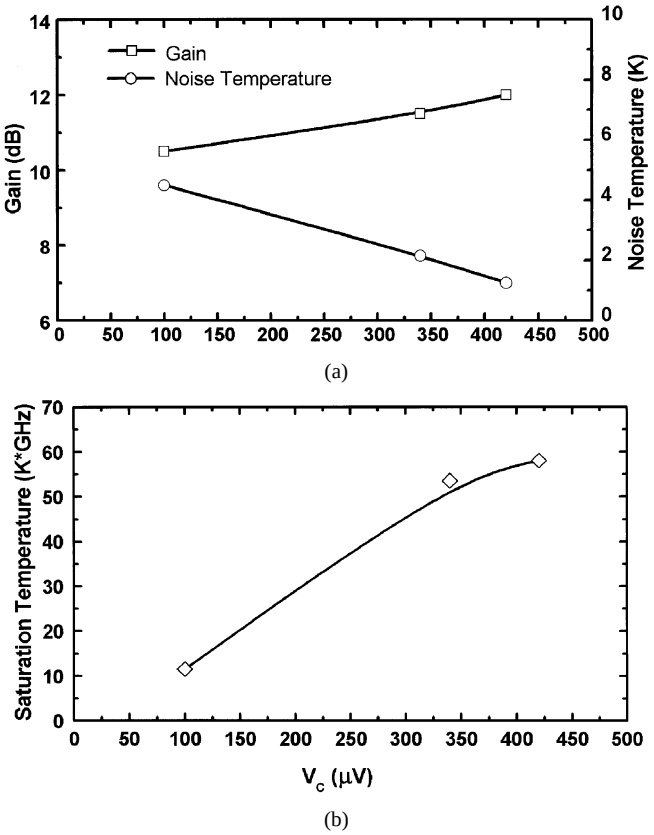

Fig. 1. (a) Noise temperature and power gain measured for LTS SQAs, (b) saturation temperature,—in the dependence on the characteristic voltage V_C.

II. Influence of Characteristic Voltage

Recently we have investigated the influence of the characteristic voltage V_C on the dynamic characteristics of 4 GHz amplifiers based on LTS dc SQUIDs [2], [3]. Fig. 1 demonstrates that increase of the characteristic voltage slightly increases the power gain and dramatically improved the noise temperature. This is in good agreement with theoretical prediction [7]. It is known that performance of SQUID can be affected by presence of resonances within input and/or output circuits. We have found such resonant conditions within the output filters. The effect of resonances is seen as current steps at the I-V curve of the SQA, thus limiting the voltage span and affecting both the

Manuscript received August 4, 2002. This work was supported in part by the Russian SSP "Superconductivity," RFBR Project 00-02-16270, the ISTC Project # 2445, the INTAS Project 01-0367, the INTAS Project 01-0809, the Hartmann Foundation, and the Danish Natural Science Council.

G. V. Prokopenko, S. V. Shitov, and I. V. Borisenko are with the Institute of Radio Engineering and Electronics, Russian Academy of Sciences, 101999, Moscow, Russia (e-mail: georgy@hitech.cplire.ru).

J. Mygind is with the Department of Physics, Technical University of Denmark, DK-2800 Lyngby, Denmark (e-mail: myg@fysik.dtu.dk).

Digital Object Identifier 10.1109/TASC.2003.814147

output power and the signal response of the amplifier [3]. This is why saturation level is difficult to handle in a practical design. To solve this problem, we try to push forward the systematic study of rf circuitry for SQAs.

By neglecting for instance the parasitic resonances in the output circuit we can estimate the maximum possible saturation temperature of the SQA. Using formula [5] for the optimal bias point of a SQUID: $V_B \approx (I_B R_N/2)\cdot(1-(I_C/I_B\cdot\cos(\pi\cdot\Phi_B/\Phi_0))^2)^{0.5}$, where Φ_0 and Φ_B are the flux quantum and the bias flux correspondingly, and I_B is the bias current, we find that for $\Phi_B \approx \Phi_0/4$ and $I_B \approx I_C$ the optimum bias voltage is $V_B \approx I_C R_N/3 \approx V_C/3$, that is somewhat lower that desirable value of $V_C/2$ estimated above. The *maximum* saturation temperature can then be estimated as $T_{\rm SAT}^{1\ \rm GHz} \approx (I_C R_N/3)^2/(8R_D \cdot k_B \cdot \Delta f \cdot G_{\rm SQA})$. Using the following parameters of HTS SQA: $G_{\rm SQA} = 12$ dB, $R_D = 50\ \Omega$ and $V_C = 5$ mV, it is possible to attain the saturation level in the range of about 1000–5000 K that is compatible with the coolable HEMT amplifiers optimized for a low-signal operation.

III. Design of SQA

A. Microwave Design

The basics for microwave design of the X-band HTS SQA with resonant input circuit is described elsewhere [1]. The proposed input resonator contains planar capacitors $C1$–$C4$ and slot-line inductors as shown in Fig. 2(a). The pares of series capacitors $C1, C2$ and $C3, C4$ are formed in the wiring layer, which is insulated from a HTS base layer and can be made not from a superconductor, but from a normal metal, e.g., Al, Au, Pt, etc. This coupling circuit can be called 'direct coupling scheme' since the resonant circuit and a part of the SQUID loop have a common current path formed in the HTS base layer. The Josephson junctions are formed at the bicrystal grain boundary (see Fig. 2(b)). The *direct* rf coupling between the input resonance circuit and the output coplanar waveguide can be very low (ideally zero), unless the two junctions are essentially unequal. The part of the input circuit containing a tuning slot line stub and capacitors $C3$ *and* $C4$ plays an important role in adjustment of input impedance of SQA and its bandwidth.

B. Gain and Noise Temperature Estimation

A small signal of flux intensity Φ_E at the frequency f_S in the SQUID inductance $L_{\rm SQA}$, corresponds to an absorbed input power of $P_{\rm IN} = \Phi_E^2/(f_S \cdot L_{\rm SQA})$ [8]. The output voltage across the dynamic resistance R_D will be $V_\Phi \cdot \Phi_E$, where the voltage responsivity V_Φ is defined as $V_\Phi = \partial V/\partial\Phi_E$. An output power can be estimated for the matched case as $P_{\rm OUT} = (V_\Phi \cdot \Phi_E)^2/R_D$. The gain will be $G = P_{\rm OUT}/P_{\rm IN} = (V_\Phi^2 \cdot L_{\rm SQA})/(f_S \cdot R_D)$. Since the voltage response to a small variation $\partial\Phi_E$ of the external flux is given by $\partial V/\partial\Phi_E \approx R_D/2L_{\rm SQA}$, the power gain can be then estimated as $G \approx R_D/(4 \cdot f_S \cdot L_{\rm SQA})$. For $f_S = 11$ GHz, $R_D \approx 50\ \Omega$ and $L_{\rm SQA} \approx (25\text{–}150)$ pH, the power gain can be estimated as 10–16 dB. The SQA noise temperature is defined in [9] as $T_N(f) \approx 2f \cdot \varepsilon(f)/k_B$, where ε is the energy resolution (per unit bandwidth). For frequencies much less than the Josephson frequency $f_J = I_C R_N/\Phi_0$ the energy resolution $\varepsilon(f) \approx 9k_B \cdot T \cdot L_{\rm SQA}/R$ and the prediction of the SQA noise temperature is $T_N(f) \approx 18 f_S \cdot T \cdot L_{\rm SQA}/R$. Assuming $T = 4.2$ K, and $\beta_L = 2L_{\rm SQA}I_C/\Phi_0 \approx 1$, we find that $T_N \approx 4$–25 K. This noise temperature is somewhat better than one of a typical cooled HEMT amplifier at 10 GHz. Note that unlike for the HEMT-amplifiers, cooling of SQA can reduce its noise temperature linearly with temperature down to values close to the quantum limit [10].

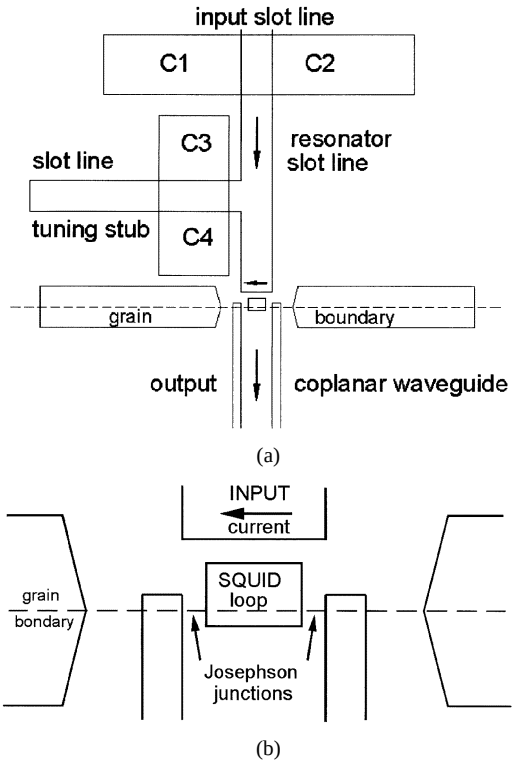

Fig. 2. Proposed HTS SQA layout with improved tuning input. (a) total view, (b) the central part.

IV. Modeling and Simulation of the SQA

A. Microwave Model for the LTS SQA

To confirm our approach in modeling SQA, we are referring to earlier experiments with LTS SQA [2]. The equivalent schematic of LTS SQA is presented in Fig. 3, where CPW_*1* is the input/output coplanar waveguide with an impedance of about 50 $\Omega, C1$ and $C2$ are input tuning capacitors, $L_{\rm COIL}$ is the inductance of the input coil, $L_{\rm SQA}$ is the inductance of SQUID loop, L_j is the junction's Josephson inductance, C_j is the capacitance of SIS junctions, $R_{\rm SH}$ is the shunt resistance, CPW_*2* is the high impedance coplanar waveguide of an output balanced filter, MSL is the microstrip stub of the filter. The element CCCS presents a Current Controlled Current Source, which *input* impedance is equal to the impedance of the SQUID loop circuit, the *output* impedance is equal to R_D, and the current gain is equal one.

For the analysis and simulation of the SQA characteristics the numerical model is suggested based on the schematic from Fig. 3. We assume as a basic approach that input impedance of the SQUID loop is related to the impedance of the signal-induced

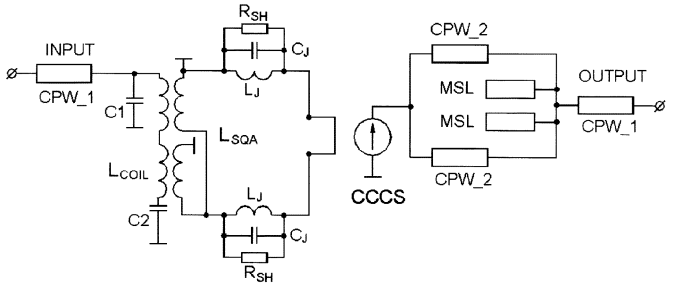

Fig. 3. The equivalent schematic of LTS SQA.

current circulating in its loop. The complete theoretical analysis of the input impedance is complicated and consequently we employ the approximation used in [7]. The input SQUID admittance for a small signal at frequency ω_S is defined as a complex coefficient $Y_i(\omega_S)$ according to the following equations: $(I_L)\omega = Y_i(\omega_S)V_\omega, V_\omega = j\omega_S(\Phi_{\rm ex})_\omega$. Here $\Phi_{\rm ex}$ is the amplitude of the input flux, which cause variation of the circulating current I_L. For low frequencies $(f_S \ll f_J)$ it can be limited to two basic terms: $Y_i(\omega_S) \approx 1/(j\omega_S L_i) + 1/R_i$, which are the input inductance and conductance of the SQUID. To find the input inductance, it is possible to calculate the derivative $L_i^{-1} = \partial I_L/\partial\Phi_{\rm ex}$, and for a low-inductive SQUID we get the following expression [7]:

$$\frac{1}{L_i} = -\frac{2\pi}{\Phi_0}\left(\frac{I_{C-}I_{C1}I_{C2}\left[1 - I_M^2/I_{C+}^2 - 2v(1+v)\right]}{2v(i+v)^2 I_{C+}^2}\right) \quad (1)$$

Here the total SQUID critical current is presented by $I_M^2 = I_{C1}^2 + I_{C2}^2 + 2I_{C1}I_{C2}\cos\varphi_{\rm ex}; v = V_B/V_C; i = I_{\rm ex}/I_M(\varphi_{\rm ex}), I_{C1}$ and I_{C2} are the critical currents of the two Josephson junctions. The 'external phase' is defined as $\varphi_{\rm ex} = 2\pi\Phi_{\rm ex}/\Phi_0$. Maximum values of the critical current $(I_M)_{\max} = I_{C+}$ takes place at the magnetic flux bias $\Phi_{\rm ex} = n\cdot\Phi_0$, and the minimum values $(I_M)_{\min} = I_{C-}$ can be found at $\Phi_{\rm ex} = (n+1/2)\cdot\Phi_0$. The total current through the SQUID is expressed as $I_{\rm ex} = I_M\sin\psi$, where the 'average phase' ψ of the interferometer is defined by the expression $\psi = \varphi_1 + \eta = \varphi_2 + \eta - \varphi_{\rm ex}$. Here φ_1 and φ_2 are the phases of the two junctions, and the parameter η can be calculated from the expression $\eta = -[2I_{C1}tg(\varphi_{\rm ex}/2)]/[I_{C+} + 2I_{C-}tg^2(\varphi_{\rm ex}/2)])$, which can be transformed as $\psi = \varphi_1 - \varphi_2 = -\varphi_{\rm ex}$. The last expression means that the 'average phase' is just opposite to the 'external phase'. To find the active component $1/R_i$ using assumption of small inductance, we can use equation [7]:

$$\frac{1}{R_i} = \frac{I_{C1}I_{C2}}{V_C I_{C+}}\left(1 - \frac{\left(I_{C+}^2 - I_M^2\right)\left[\cos^2(\varphi_{\rm ex}/2)\right] + v(v+1)}{I_{C+}^2 v^2 (i+v)^2}\right) \quad (2)$$

Substituting in these expressions (1)–(2) parameters that could be realized experimentally, we find the following numerical estimations: $L_i \approx 25$ pH, $R_i \approx 17\ \Omega$. To complete the calculation, the inductance of the SQUID loop has to be added to the loop impedance. The active component appears rather close to the sum of shunts resistance, $R_i \approx 2\cdot R_{\rm SH}$ (resistance of the shunt $R_{\rm SH} \approx 8\ \Omega$ [2]), and the inductive component, is approximately equal to twice the Josephson inductance [11], $L_J \approx \Phi_0/(2\pi I_C(1 - (I_B/I_{C1,2})^2)^{0.5}), L_J \approx 13.7$ pH. Here I_B is the dc current bias, and $I_{C1,2}$ the critical currents of junctions. Now it is possible to present the equivalent circuit of the SQUID loop, as a series connection of three elements: the loop inductance and two junctions, each presented by L_J in parallel with the shunt resistance $R_{\rm SH}$. The current gain of the SQA can be calculated from the flux-current transfer function $J_\Phi = V_\Phi/R_D$. Here V_Φ is the flux-voltage transfer characteristic $V_\Phi \approx R_D/L_{\rm SQA}$. The gain approximation can be written as $G_I \approx J_\Phi L_{\rm SQA} Qk^2$. Here Q is the quality factor of the input contour, $k-$coupling coefficient, and $Qk^2 \approx 1$ is the parameter determining the transfer of power within the input resonance circuit. A realistic estimation gives value $G_I \approx 1$, i.e., no current gain is expected. Finally, the output impedance can be assumed just to be equal to the dynamic resistance of the I-V curve, R_D, which value can be measured (estimated) using the experimental (model) I-V curve. As a conclusion we note the good agreement between simulated and experimental values [2] as presented in Fig. 4.

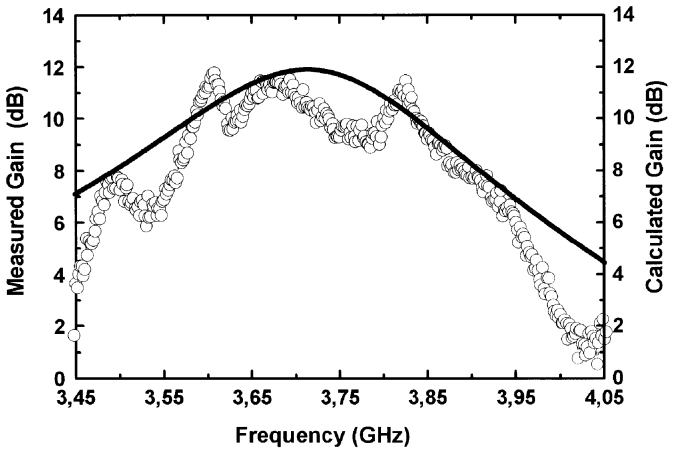

Fig. 4. The measured (◯) and calculated (_) LTS SQA power gain.

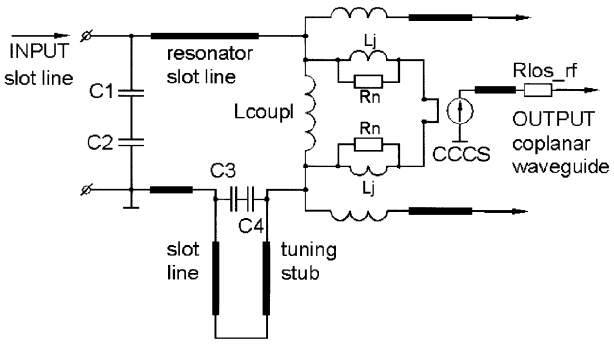

Fig. 5. The equivalent circuit of the HTS SQA.

B. Microwave Model for HTS SQA

Since the approach described above appears adequate for LTS SQA, we use it also for simulation of HTS SQA. The equivalent circuit of HTS SQA is presented in Fig. 5. The coupling inductance $L_{\rm COUPL}$ was chosen to be about 50 pH that is a practical layout estimate.

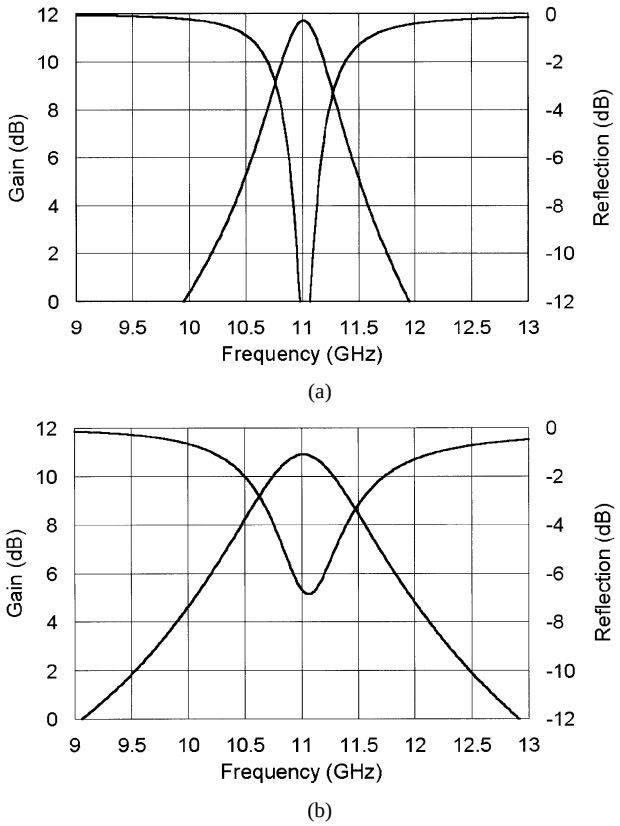

Fig. 6. Calculated power gain and the input reflection loss. Simulations are made for different goals: (a) is the best coupling at central frequency, and (b) for improved bandwidth.

The characteristics simulated for HTS SQA are presented in Fig. 6. The data from Fig. 6(a) are calculated for the goal of best coupling (lowest reflection loss). This set of parameters provides relatively narrow bandwidth of approximately 500 MHz. It is shown at the bottom diagram (see Fig. 6(b)) that a wider bandwidth of approximately 1 GHz can be achieved as a trade-off between the gain and the reflection loss.

V. Conclusion

We have suggested a new concept for design of an X-band amplifier based on a HTS dc SQUID with saturation power sufficient for practical applications. This opens the possibility for further increase in both saturation power and bandwidth of the amplifier. Present research can be a good basis for future development of a practicable amplifier for IF processing and satellite communication.

Acknowledgment

The authors would like to thank V. P. Koshelets, K. I. Constantinian, and G. A. Ovsyannikov for fruitful discussions.

References

[1] G. V. Prokopenko, S. V. Shitov, I. V. Borisenko, and J. Mygind, "HTS dc SQUID based rf amplifier: Development concept," *Physica C*, vol. 368/1-4, pp. 153–156, 2002.

[2] G. V. Prokopenko, S. V. Shitov, D. V. Balashov, P. N. Dmitriev, V. P. Koshelets, and J. Mygind, "Low-noise S-band DC SQUID amplifier," *IEEE Trans. on Appl. Supercond.*, vol. 11, pp. 1239–1242, Mar. 2001.

[3] G. V. Prokopenko, S. V. Shitov, I. L. Lapitskaya, V. P. Koshelets, and J. Mygind, Dynamic Characteristics of S-Band DC SQUID Amplifier. in this volume.

[4] P. N. Dmitriev, I. L. Lapitskaya, L. V. Filippenko, A. B. Ermakov, S. V. Shitov, G. V. Prokopenko, S. A. Kovtonyuk, and V. P. Koshlets, High Quality Nb-Based Integrated Circuits for High Frequency and Digital Applications. in this volume.

[5] R. Gross *et al.*, "SQUIDS employing high T_C superconductors," in *Principles and Applications of Superconducting Quantum Interference Devices*, A. Barone *et al.*, Ed: World Scientific, 1992, pp. 420–472.

[6] U. Poppe, Y. Y. Divin, M. I. Faley, J. S. Wu, C. L. Jia, P. Shadrin, and K. Urban, "Properties of Y $Ba_2Cu_3O_7$ thin films deposited on substrates and bicrystals with vicinal offcut and realization of high $I_C R_N$ junctions," *IEEE Trans. Appl. Supercond.*, vol. 11, no. 1, pp. 3768–3771, Mar. 2001.

[7] K. K. Likharev, *Dynamics of Josephson Junctions and Circuits*: Gordon and Breach Science Publishers, 1986.

[8] P. Carelli *et al.*, "Macroscopic quantum interference: DC-SQUID," in *Principles and Applications of Superconducting Quantum Interference Devices*, A. Barone *et al.*, Ed: World Scientific, 1992, pp. 3–75.

[9] J. Clarke, *SQUID Fundamentals. SQUID Sensors: Fundamentals, Fabrication and Application*, H. Weinstock, Ed: Kluwer Academic Publishers, 1996, pp. 1–62.

[10] M. Mueck., J. B. Kycia, and J. Clarke, "Superconducting quantum interference device as a near-quantum-limited amplifier at 0.5 GHz," *Appl. Phys. Lett.*, vol. 78, no. 7, pp. 967–969, 2001.

[11] P. O. Terry and A. D. Kevin, "Foundation of applied superconductivity," Massachusetts Institute of Technology, Addison-Wesley Publishing Company, 1991.